FIRST DEMONSTRATION OF A ZrNb ALLOYED SURFACE FOR SUPERCONDUCTING RADIO-FREQUENCY CAVITIES *

Z. Sun[†], M. U. Liepe, T. Oseroff[‡]

Cornell Laboratory of Accelerator-Based Sciences and Education, Ithaca, NY 14853, USA

Abstract

RF surface design is a promising path to next-generation SRF cavities. Here, we report a new strategy based on ZrNb surface alloying. Material development via an electrochemical process is detailed. RF performance evaluated in the Cornell sample test cavity is discussed. Cornell demonstrates that ZrNb alloying is a viable new technology to improve the performance of SRF cavities.

INTRODUCTION

To boost the performance of superconducting radio-frequency (SRF) cavities, we are motivated to search for next-generation materials and surfaces, together with advanced methods to produce such surfaces. Recently, our theory collaborators at the Center for Bright Beams predict that ZrNb alloys allow large enhancement of the critical temperature and superheating field as compared to conventional niobium [1]. The work we present here aims to provide the experimental demonstration of a ZrNb alloyed SRF cavity.

ZrNb random alloys have been investigated decades ago [2], but the highest T_c reported (11 K) is lower than the theoretical prediction of 18 K T_c for either ordered cubic ZrNb [1, 3] or bcc Zr [4]. Also, thin film ZrNb samples made by sputtering showed T_c of 7.4 K [5]. One of the most critical factors to ensure a high T_c in the ZrNb system is maintaining the desirable cubic structure. Thus, the material design that induces cubic, ordered ZrNb alloys along with a maximized T_c is one goal of this work.

Moreover, ZrNb alloys have not been studied on the cavity scale yet. Calculations showed the addition of Zr in Nb could enable a 1.8 times improvement in the superheating field, a parameter that determines the maximum accelerating gradient for SRF applications [1, 6]. Developing the fabrication process of ZrNb cavities and evaluating their RF superconducting properties are necessary and novel.

We, at Cornell, are establishing the electrochemical deposition technique for surface-alloyed cavities [7–9]. The benefits include an inner-surface facilitated process that is compatible with a complicated 3-D cavity structure, in addition to some unique material products owing to the electrochemical reactions.

Here, we report the fabrication and characterization of electrochemically made ZrNb samples. We observed cubic Zr-Nb surfaces that show T_c values exceeding literature values of ZrNb random alloys. Also, we report the RF performance of ZrNb-alloyed surface in a test cavity. We show the improved BCS resistance of the alloyed sample owing to the high T_c phase as compared to the baseline Nb. Note that a thorough analysis can be found in Ref. [10].

METHODS

A three-electrode electrochemical deposition system was used to deposit Zr films on the Nb surface in an inert gas glovebox. Fig. 1a shows the setup used for process optimization on the sample scale. Pt counter, Nb working, and pseudo reference electrodes were employed together with a hotplate with temperature feedback control. We optimized precursor concentration, deposition temperature, electrochemical potential, and deposition time.

Before Zr deposition, Nb substrates were electropolished with a nominal 100 μm removal. These substrates were HF soaked to remove surface oxides and impurities before any deposition in the glovebox. ZrNb samples were made through the electrochemical reaction under 2 – 10 hours duration. These samples were subsequently annealed in the furnace under 10^{-7}–10^{-6} Torr vacuum.

Material characterization was performed. X-ray photoelectron spectroscopy (XPS) was used to determine the Zr depth profiles, while energy dispersive X-ray spectroscopy (EDS) imaging was performed to preliminarily confirm the elemental information. High resolution X-ray diffraction (Rigaku XRD) was used to identify the crystal phase. Scanning electron microscopy (Zeiss Gemini 500 SEM) was used to probe the surface morphology.

After the electrochemical and annealing conditions were optimized, we scaled up the process to sample sizes used with the Cornell TE-mode sample test cavity [11] for measuring surface resistances and quench fields at 4 GHz and 5.2 GHz. We measured the critical temperature using two
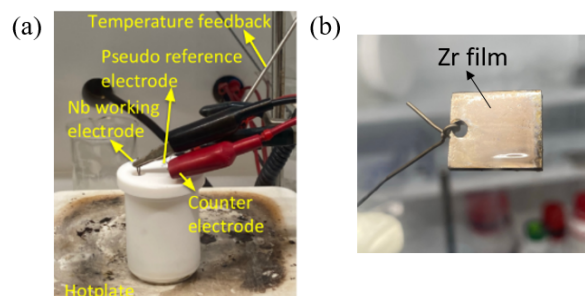

Figure 1: (a) Three-electrode setup for Zr electrochemical deposition at Cornell. (b) Picture of the electrochemically fabricated Zr film on a Nb surface.

methods: a four-probe measurement via the Quantum Design Physical Property Measurement System (PPMS) under the AC transport mode, and a flux expulsion test during warming the cryostat slowly.

RESULTS AND DISCUSSION

Material Study Using Electrochemical Deposition

Figure 1b shows the ZrNb sample image taken immediately after a 4 hours electrochemical reaction in the inert-gas glove box. We find the Zr deposition is able to induce reaction between Zr precursor and Nb surface. As evidenced by the XPS spectra, in Fig. 2, ZrNb alloys are formed after the reaction. Such Zr reduction is confirmed by the cyclic voltammetry. However, both XPS and EDS spectra showed the presence of unwanted impurities partially induced during the deposition.

After thermal annealing, as shown in Fig. 2, we observe the binding energy shifting toward the metallic positions, e.g., for both Zr and Nb 3p photoelectrons. This behavior accompanies with the disappearance of the impurities that are responsible for no observation of superconducting transition in as-deposited samples. By contrast, oxygen and carbon intensities are significant. We notice oxygen atoms merely exist in a wide-bandgap zirconium dioxide which works well with SRF applications. The carbon motif is still a puzzle that is being solved.

Locking an ordered, cubic crystal phase is essential in this work as detailed in Ref. [1]. Our XRD data show either diffraction peaks or peak shoulders that appear next to the bcc Nb diffractions. This is a clear evidence for ZrNb cubic shifting that obeys the Vegard's law. The shifting is led by a larger lattice parameter of bcc Zr (0.354 nm [12]) than Nb. We are able to avoid the unwanted hexagonal Zr phases that are stable under an equilibrium processing condition but result in low T_c values [4]. However, the phase transformation mechanism is complicated when four elements are involved. To pursue a conclusive answer, we are correlating our X-ray diffraction data with insights from local electron diffraction performed by Zhaslan Baraissov in Prof. David A. Muller's group.

PPMS resistance measurements show a 13 K superconducting transition for thick ZrNb films that were produced by long electrochemical reaction time, whereas flux expulsion measurements suggest an even higher T_c, 16 K, on a cavity-scale test using a thinner film. We clarify our understanding on three aspects. First, our measured values are higher than the 11 K ZrNb random alloys [2] and the 7.4 K T_c sputtered films [13]. Theoretical calculations in Ref. [1] explained the fundamental limit of T_c for ZrNb alloys. Meanwhile, we are analyzing other possible functional phases existing in our four-element system. Second, the T_c difference between sample measurement using PPMS and cavity measurement using flux expulsion is likely due to a different Zr profile resulted from a low current density during cavity-scale deposition. Third, although our films made by short reaction time did not show a clear superconducting transition, the
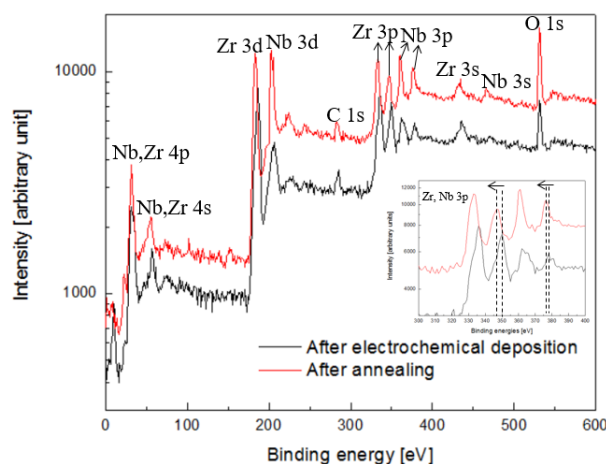

Figure 2: X-ray photoelectron spectra after electrochemical deposition and after thermal annealing, showing the formation of ZrNb alloys.

wire bonding on these thin films for PPMS may strongly affect their measurements.

RF Evaluation of a ZrNb Cavity

Figure 3 shows the scaling up results of electrochemical deposition on a test plate in the Cornell TE-mode sample test cavity. Before Zr deposition, in Fig. 3a, the film host plate was baked at 800 °C and 5 μm electropolished. We observe slight color contrast on the plate surface after ZrNb alloying (Fig. 3b).

During the cavity plate deposition, cyclic voltammetry results matched with the sample-scale study. We used the same chemical ratio and reduction potential, while we noticed the current density was seven times smaller than that used for sample study under the same condition. This is likely due to the current limitation from thin electrodes used. This difference affects the Zr surface profile, and cutout samples are prepared for further investigation.

We measured the RF performance of both baseline (Fig. 3a) and ZrNb-alloyed (Fig. 3b) plates under 4 GHz and 5.2 GHz frequencies. In order to examine some uncontrolled influences from the initial surface, e.g., the scratch on the plate edge, we also include results from previous baseline tests in the data analysis.
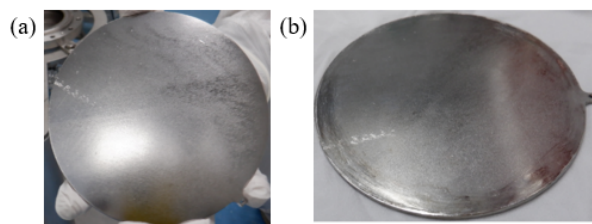

Figure 3: Scaling up the electrochemical process to Cornell sample test cavity. Pictures of the host plate (a) before Zr deposition and (b) after ZrNb surface alloying.
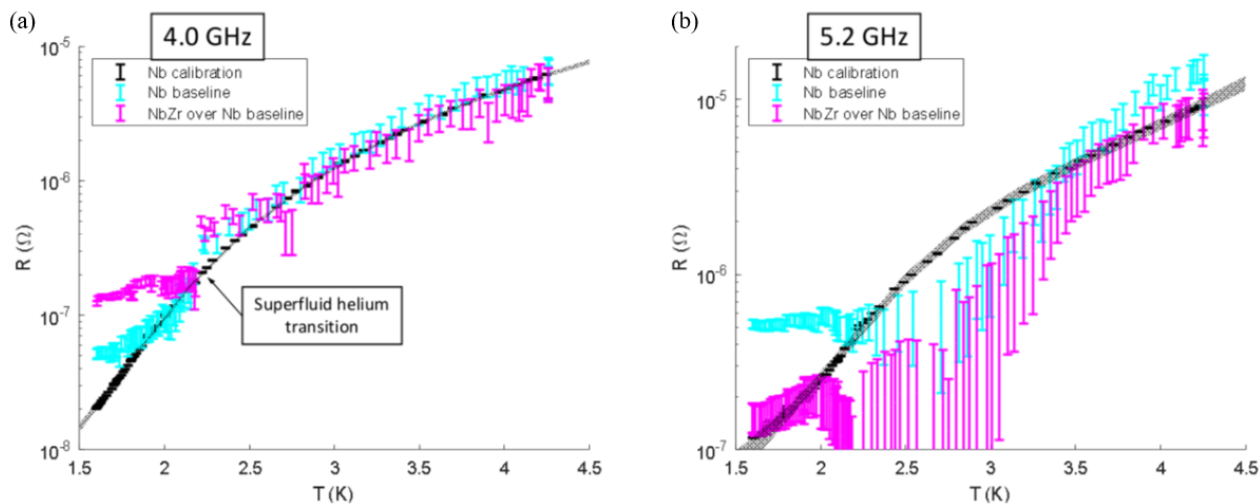
THYE6

Figure 4: Temperature dependent surface resistance measured at (a) 4.0 GHz and (b) 5.2 GHz.

Surface resistance versus temperature curves (Fig. 4) taken under a low field of 1 mT revealed a reduction of BCS resistance after ZrNb alloying. Our baseline results (blue) roughly match with previous calibration data (black), but we do observe high residual resistance on the baseline plate. When comparing ZrNb results (purple) with the baselines (blue), we find ZrNb alloys trend lower than the baseline at the high temperatures ranging from 2 K to 4 K. This trend is especially obvious under a 5.2 GHz RF condition. Moreover, the low temperature (<2 K) results are unusual. We observed ZrNb reduces residual resistance toward previous calibration values for 5.2 GHz measurements, while the alloy adds significant residual at 4 GHz measurements. We plan on more testing of new ZrNb coated cavities to explain this unclear behavior.

CONCLUSION

In summary, we developed a ZrNb alloying process via electrochemical deposition and we demonstrated cubic ZrNb surface alloys yielding critical temperature up to 16 K. We also provided the first RF result of the ZrNb-alloyed sample test cavity. The most critical finding is the reduction of BCS resistance owing to the high T_c ZrNb alloys in our cavity. This first experimental demonstration of ZrNb alloys may open a new direction for SRF cavities with high critical temperature, low surface resistance and potentially high superheating fields.

ACKNOWLEDGEMENTS

REFERENCES

[1] Z. Sun *et al.*, "Theory of Nb-Zr alloy superconductivity and first experimental demonstration for superconducting radio-frequency cavity applications", unpublished.

[2] J. M. Corsan, I. Williams, J. A. Catterall, and A. J. Cook, "Superconductor transition temperatures of zirconium-niobium alloys", *J. Less-Common Met.*, vol. 15, no. 4, pp. 437–443, 1968. doi:10.1016/0022-5088(68)90109-4

[3] N. S. Sitaraman *et al.*, "Theory results on novel surface preparations for superconducting radio-frequency cavities", presented at 2022 MRS Spring Meeting, Honolulu, HI, USA, May 2022.

[4] B. T. Wang, P. Zhang, H. Y. Liu, W. D. Li, and P. Zhang, "First-principles calculations of phase transition, low elastic modulus, and superconductivity for zirconium", *J. Appl. Phys.*, vol. 109, no. 6, p. 063514, 2011. doi:10.1063/1.3556753

[5] A. Cavalleri, F. Giacomozzi, L. Guzman, and P. M. Ossi, "Structure and superconductivity of Nb-Zr thin films", *J. Phys.: Condens. Matter*, vol. 1, no. 37, pp. 6685–6693, 1989. doi:10.1063/1.3556753

[6] B. Francis *et al.*, "Superheating field of inhomogeneous surface layers in Ginzburg-Landau theory using linear stability", unpublished.

[7] Z. Sun *et al.*, "Toward Stoichiometric and Low-Surface-Roughness Nb₃Sn Thin Films via Direct Electrochemical Deposition", presented at the SRF'21, East Lansing, MI, USA, Jun.-Jul. 2021, paper WEOTEV03, unpublished.

[8] Z. Sun *et al.*, "Electroplating of Sn Film on Nb Substrate for Generating Nb₃Sn Thin Films and Post Laser Annealing", in *Proc. SRF'19*, Dresden, Germany, Jun.-Jul. 2019, pp. 51–54. doi:10.18429/JACoW-SRF2019-MOP014

[9] Z. Sun *et al.*, "Materials investigation and surface design of superconducting radio-frequency accelerating cavities at Cornell University", presented at 2022 MRS Spring Meeting, Honolulu, HI, USA, May 2022.

[10] Z. Sun *et al.*, "Inhomogeneous surface design via ZrNb alloying for superconducting radio-frequency accelerator cavities", unpublished.

[11] T. E. Oseroff, M. Liepe, and Z. Sun, "Sample Test Systems for Next-Gen SRF Surfaces", presented at the SRF'21, East Lansing, MI, USA, Jun.-Jul. 2021, paper TUOFDV07, unpublished.

[12] G. B. Thompson *et al.*, "Phase stability of bcc Zr in Nb/Zr thin film multilayers", *Acta Mater.*, vol. 51, no. 18, pp. 5285–5294, Oct. 2003. doi:10.1016/S1359-6454(03)00380-X

[13] A. Cavalleri *et al.*, "Structure and superconductivity of Nb-Zr thin films", *J. Phys.: Condens. Matter*, vol. 1, no. 37, pp. 6685–6693, Oct. 1989. doi:10.1088/0953-8984/1/37/015